International Journal of Architectural, Civil and Construction Sciences
ISSN: 2415-1734
Vol:14, No:11, 2020

Seismic Performance Evaluation of the Composite Structural System with Separated Gravity and Lateral Resistant Systems

Zi-Ang Li, Mu-Xuan Tao

***Abstract*—**During the process of the industrialization of steel structure housing, a composite structural system with separated gravity and lateral resistant systems has been applied in engineering practices, which consists of composite frame with hinged beam-column joints, steel brace and RC shear wall. As an attempt in steel structural system area, seismic performance evaluation of the separated composite structure is important for further application in steel housing. This paper focuses on the seismic performance comparison of the separated composite structural system and traditional steel frame-shear wall system under the same inter-story drift ratio (IDR) provision limit. The same architectural layout of a high-rise building is designed as two different structural systems at the same IDR level, and finite element analysis using pushover method is carried out. Static pushover analysis implies that the separated structural system exhibits different lateral deformation mode and failure mechanism with traditional steel frame-shear wall system. Different indexes are adopted and discussed in seismic performance evaluation, including IDR, safe factor (SF), shear wall damage, etc. The performance under maximum considered earthquake (MCE) demand spectrum shows that the shear wall damage of two structural systems are similar; the separated composite structural system exhibits less plastic hinges; and the SF index value of the separated composite structural system is higher than the steel frame shear wall structural system.

***Keywords*—**Finite element analysis, seismic performance evaluation, separated composite structural system, static pushover analysis.

I. Introduction

DURING extensive applications of traditional composite frame-shear wall structure system in steel housing area, higher demand in structural design standardization and assemblage construction efficiency have been requested. In practical engineering cases, steel members and joints with complex type make it difficult for traditional steel structure to develop advantage in assemblage construction and convenient design.

For improvements of assembly steel structures, many researches have focused on integrated assembly components [1]-[3]]. Varied types of structural system also have been proposed for engineering applications based on those new components [4]-[6]]. However, those innovations in structural system generally depend on application of integrated assembly components and adjustment of member arrangement, but make little change in structural global mechanism. For further improvement in structural system, a composite structural system with separated gravity and lateral resistant systems is proposed, which has been practiced in actual engineering case located in Tangshan, China.

ZA. Li and MX. Tao are with Department of Civil Engineering, Tsinghua University, Beijing, 100084 China (e-mail: liza17@mails.tsinghua.edu.cn, taomuxuan@tsinghua.edu.cn).

The separated composite structural system typically consists of: (i) composite frame with hinged column-beam joints, performing as gravity resistant system; (ii) RC shear wall, performing as main lateral resistant member; (iii) steel brace, performing as supplement of lateral resistant member. This structural composing form presents an explicit load transmission mechanism. Each beam in the separated composite structural system behaves as simply supported beam under gravity loads because of the hinged supported boundary conditions, with no contribution to the global lateral resistance stiffness. Therefore, the design size of beam cross section can be easily determined according to static loading conditions. Uniform section size can be adopted for simplification and convenience in structural design and construction, by which the design standardization and construction assembly efficiency can be improved.

Considering the difference in lateral resistant mechanism, when subjected to seismic loads, the separated composite structural system could behave differently in lateral displacement pattern and failure mode compared to traditional composite frame-RC shear wall structural system. Therefore, the seismic response and performance of separated composite structural system is necessary to be studied.

In this paper, two structural schemes are designed and corresponding finite element models are established according to traditional composite frame-RC shear wall structural system and separated composite structural system, based on the control criteria of one same elastic IDR limit under frequent earthquake. A comparative analysis of these two systems is carried out using elastic-plastic pushover method, and their seismic performances are evaluated using varied indicators such as inter-story displacement, damage states of key components and safety factor suggested in [7]-[9].

II. Case Study: Design

A case study building is designed to frequently occurred earthquake level according to Chinese structure design provisions [10]. Then, their respective performances are assessed.

In Fig. 1, the structure prototype of 20-story high-rise building is presented. The story height is 3 m, and the span

length is 32 m (in X direction) and 17 m (in Y direction) respectively. RC shear walls are arranged in the center of the structure plane.

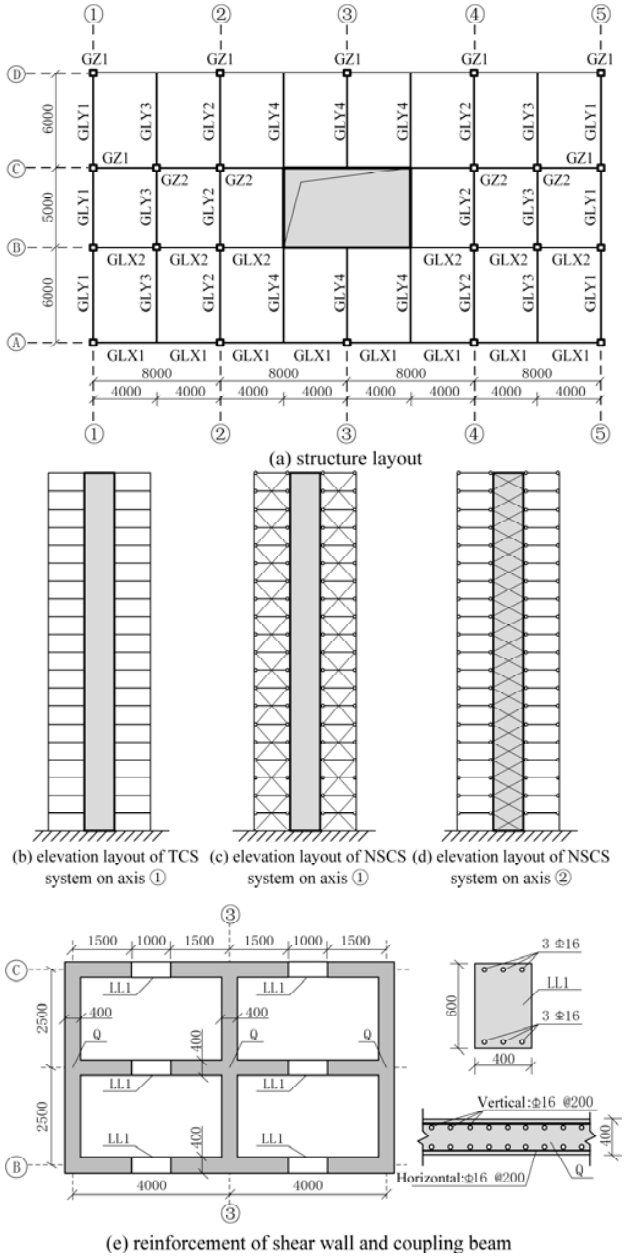

Fig. 1 Structure layout of two systems

A. Design Strategies

The prototype building is designed into two different structural systems, namely, traditional composite frame-RC shear wall structural system (TCS system) and new composite structural system with separated gravity and lateral resistant systems (NSCS system). In the design procedure, taking IDR as design criteria to control the lateral behavior under frequently occurred earthquake level, both two systems are designed with IDR value close to 1/800, which is maximum limiting value according to Chinese structure design provisions, in order to minimize cross section of members and thus avoiding unnecessary structural over strength that could affect the seismic performance of two different systems.

Concrete f_c = 50 MPa and steel f_y = 345 MPa are used. For TCS system and NSCS system, one main difference consists in boundary condition of beam-column joint. Fixed beam-column joint is considered in TCS system and hinged beam-column joint is considered in NSCS system. In TCS system, both composite frame and RC shear wall components behave as lateral resistant system whereas in NSCS system, since hinged beam-column joint results in no contribution of composite frame to global lateral stiffness, brace components behave as supplement of this part. The arrangement of brace components are presented in Fig. 1.

In both TCS and NSCS system, the slab spatial composite effect on composite beam is considered using equivalent concrete slab width. In TCS system, with fixed beam-column joint, the equivalent concrete slab width of composite beam is calculated according to provisions of fixed continuous composite beam in JGJ 138-2016, Chinese code for design of composite structures [11]. In NSCS system, with hinged beam-column joint, the equivalent concrete slab width of composite beam is calculated according to provisions for composite beam with hinged boundaries in JGJ 138-2016.

Related seismic design conditions are determined based on geographic location of prototype building and Chinese seismic design provisions, including the classification of design earthquake (Group I), seismic fortification intensity (8 degree), design earthquake fundamental acceleration value (0.20g), and design characteristic period (0.35s). Finite element analysis software *Midas.Gen* is adopted for structure design.

B. Results of Design

In Tables I and II, characteristics of beam components in two structural systems are summarized, being b_f the width of steel flange, t_f the thickness of steel flange, h_w the height of steel web, and t_w the thickness of steel web. In both two systems, columns are concrete filled steel tubular cross section, being 900×900 mm for GZ1 with 20 mm thickness of steel tube, and 800×800 mm for GZ2 with 16 mm thickness of steel tube, and design characteristics of RC shear wall and coupling beam components are illustrated in Fig. 1 (e). Steel brace components in NSCS system are 200×300 mm rectangle tubular cross section with 20 mm thickness of steel tube.

TABLE I
DESIGN SIZE OF BEAM CROSS SECTIONS OF TCS SYSTEM

Component	b_f/mm	t_f/mm	h_w/mm	t_w/mm
GLY1	270	14	472	14
GLY2	200	12	426	14
GLY3	250	14	472	14
GLY4	200	14	422	16
GLX1	200	14	222	14
GLX2	200	14	252	14

Symmetric I-section is adopted for all steel beam cross sections. Equivalent width of concrete slab is calculated by provisions of fixed continuous composite beams in JGJ-138-2016 [11].

TABLE II
DESIGN SIZE OF BEAM CROSS SECTIONS OF NSCS SYSTEM

Component	b_f/mm	t_f/mm	h_w/mm	t_w/mm
GLY1	220	12	256	14
GLX1	200	12	206	12

Design cross section sizes are the same relatively for beams in X and Y direction.

Symmetric I-section is adopted for all steel beam cross sections. Equivalent width of concrete slab is calculated by provisions of simply supported composite beams in JGJ-138-2016 [11].

In NSCS system, because of the unique lateral resistant mechanism explained in Section II *A*, the composite beams behave as simply supported beam and only vertical loads are considered in design loads. As a result, cross section design results of composite beam in X and Y directions are respectively the same whereas in TCS system, design results are different because both vertical and lateral loads must be calculated in frame beams. In terms of assembly structural system, this simplification in cross section design in NSCS system brings significant improvements in design and construction stage.

Fig. 2 presents the IDR distributions of two systems under frequently occurred earthquake level in Y direction. Maximum design IDR value of two systems are within the 1/800 limit, being 1/806 (3.72 mm) for TCS system and 1/801 (3.74 mm) for NSCS system.

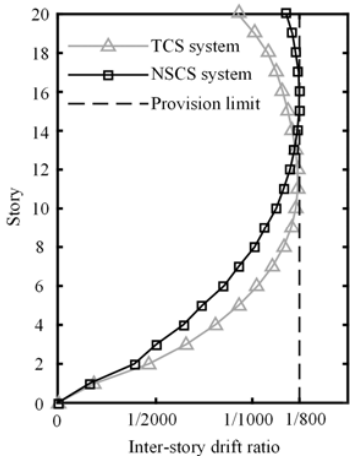

Fig. 2 IDR distribution of two systems in Y direction

C. FE Modelling Strategies

Based on the design results, FE models of two systems are established using finite element analysis software *MSC.Marc* 2014. Line shape components like composite beam, column, steel brace and RC coupling beam, are simulated by beam elements using a modified fiber beam-column element in the subroutine package *COMPONA-MARC*. The accuracy of the modified fiber beam-column element in nonlinear analysis of composite frame systems has been substantially validated [12], [13]. RC shear wall components are simulated by layered shell elements in *MSC.Marc* program, suggested by [14].

For material properties, the constitutive curve suggested by [15] is adopted as the uniaxial stress-strain skeleton curve of the concrete slab, and the constitutive curve suggested by [16] is adopted as the uniaxial stress-strain skeleton curve of steel. Detailed parameters of two constitutive curves are listed in Fig. 3.

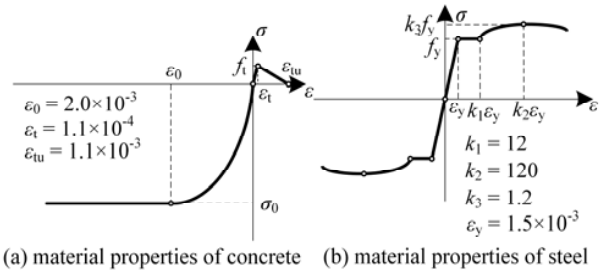

(a) material properties of concrete (b) material properties of steel

Fig. 3 Stress-strain curves of concrete and steel

In FE model, the assumption of floors as horizontal rigid diaphragms is adopted, therefore X-Y plane degree of freedom of all nodes in the composite floor plane are associated using RBE2 boundary condition in each story.

TABLE III
VIBRATION CHARACTERISTIC COMPARISON OF FE MODELS

System	FE model	Natural vibration period T/s		
		1_{st} order	2_{nd} order	3_{rd} order
TCS	*Midas*	1.5518	1.5251	1.4405
	Marc	1.6281	1.5262	1.4043
Relative error %		4.92	0.08	2.51
NSCS	*Midas*	1.7501	1.4697	1.1067
	Marc	1.7103	1.5926	1.0885
Relative error %		2.28	8.36	1.65

The calculation accuracy of FE models is verified by comparing the vibration characteristic values of *Midas.Gen* and *MSC.Marc* FE models. Modal analysis results of *Midas.Gen* and *MSC.Marc* models are similar, being flexural mode in X and Y direction for first and second order, and torsional mode in Z direction for third order, and structure frequency results in each order are also close, as presented in Table III.

III. STATIC PUSHOVER ANALYSIS

In this section, using *MSC.Marc* models of traditional composite structural system and new separated composite structural system, nonlinear static analysis ("pushover", SPO) is carried out. By SPO analysis, the lateral deformation pattern and plasticity development mechanism of the NSCS system are studied compared to TCS system. Seismic performance is also evaluated by spectrum analysis using demand spectrum under medium earthquake (Design based earthquake, DBE) and MCE level.

A. SPO Analysis

The SPO analysis is carried out with subroutine developed by [17], by which specific lateral load patterns can be applied on the structure. In this study, a lateral load pattern of "MODE" is considered, proportional to modal displacement and masses. Considering a uniformly distributed story mass, the lateral

force subjected to each story is determined as follows:

$$\Delta F_i = \phi_{2i} \Delta V_b$$

where ϕ_{2i} is the relative modal displacement of 2_{nd} order at i_{th} story; ΔV_b is the structure base shear force increment. Considering the Y direction pushover condition, the 2_{nd} order vibration mode is adopted as corresponding modal pattern.

In Fig. 4, pushover curves are plotted. The global lateral stiffness of TCS and NSCS system are close at elastic stage, and decreases with the increase of lateral force and structural plasticity development. Generally the TCS system presents a higher lateral stiffness in plastic stage compared to NSCS system implied by pushover curves. Detailed analysis of structure behavior during SPO analysis of two systems is presented in Section III *B*.

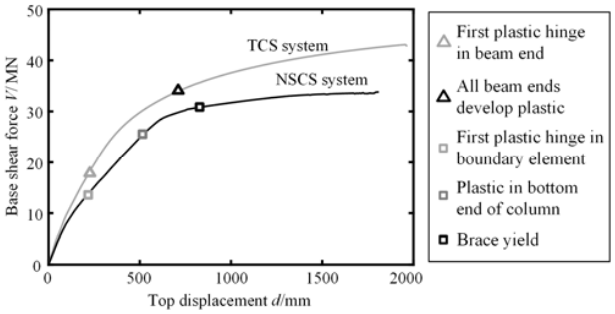

Fig. 4 Pushover curves of two systems

B. Structure Behavior

During pushover stage, the lateral deformation of TCS and NSCS system are presented in Fig. 5. For high-rise buildings with frame-shear wall system, global lateral deformation is a combined result of lateral deformations from frame and shear wall systems. For TCS system, lateral resistant stiffness of composite frame is considerable; therefore its global lateral deformation pattern is close to shear-flexural type. For NSCS system, the lateral resistant stiffness of composite frame is neglected because of the hinged beam-column joint, implying that the frame system has no contribution in global lateral deformation constraint. The global lateral deformation pattern, which is generally determined by shear wall system, is typically flexural type.

Significant plasticity development states are plotted in Fig. 4. The ultimate plasticity distribution of TCS and NSCS systems is presented in Fig. 6. In TCS system, during the pushover stage, all plastic hinges exist in beam ends of composite frame system, which is consistent with general plasticity pattern of frame-shear wall structural system. In NSCS system, since beams are designed as simply supported beam, structural plasticity mainly exists in column ends rather than beam ends. Structure plastic hinges firstly appear in confined boundary elements in bottom of the shear wall, and mainly exists in the bottom end of columns in bottom story. With the increase of lateral pushover force and damage accumulation, in bottom story, all columns produce plastic hinges at bottom end and some braces also yield.

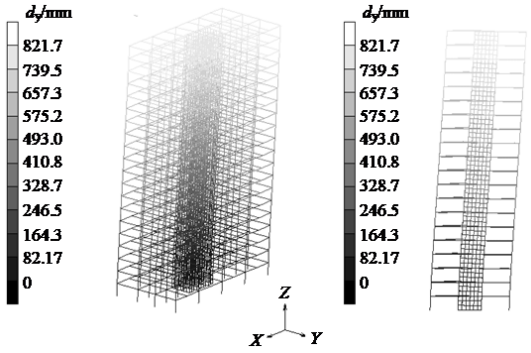

(a) TCS system

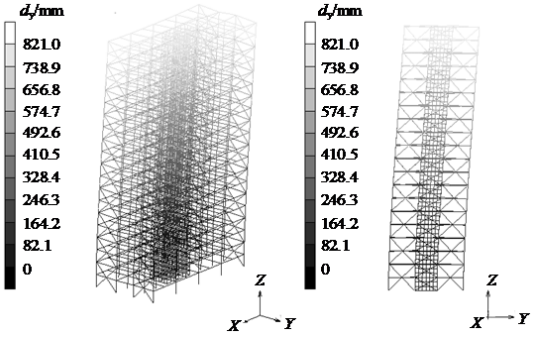

(b) NSCS system

Fig. 5 Lateral deformation in Y direction of two systems

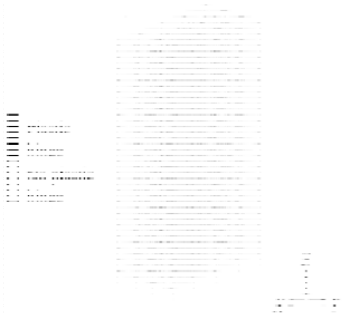

(a) TCS system

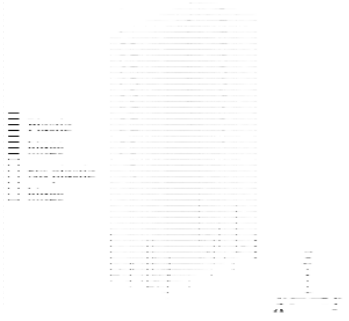

(b) NSCS system

Fig. 6 Distribution of plastic hinges of two systems

By comparison, conclusions focusing on NSCS system can be obtained: relative less plastic hinges are produced in structure; plasticity exists in column ends and braces, and beams remain elastic during pushover stage; structure failure state is later than TCS system, indicating a higher capacity under lateral force.

C. Spectrum Analysis Results

In this section, deformation spectrum response is calculated. Capacity curves are developed according to capacity spectrum method in ATC-40 [18] and [19], and elastic horizontal demand acceleration spectrum under DBE and MCE levels suggested by GB50011-2010 [10], as presented in Fig. 7 (a). It can be learned that both two systems perform obvious plastic response under MCE level, therefore a reduced plastic demand spectrum for MCE level should be considered. By equivalent damping method suggested in FEMA 273/274 [20], [21], reduced plastic demand spectrum is developed, as shown in Figs. 7 (b) and (c).

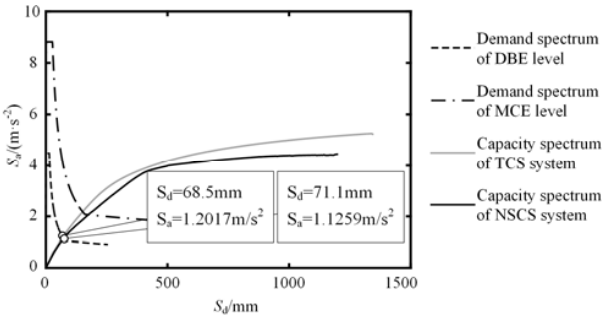

(a) Elastic demand spectrum curves of DBE and MCE levels

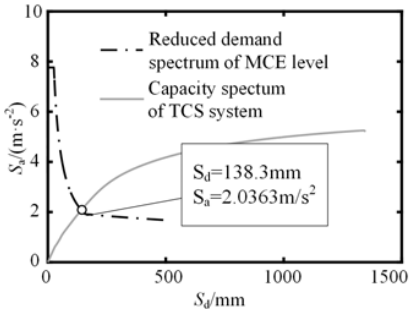

(b) Inelastic demand spectrum and capacity curve of TCS system

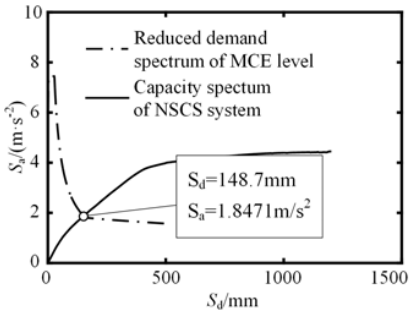

(c) Inelastic demand spectrum and capacity curve of NSCS system

Fig. 7 Demand and capacity curves of two systems

Spectrum responses of two systems under DBE and MCE levels are respectively illustrated in Fig. 7. Under MCE level, corresponding deformation response of structures is:

- $d_{1,\text{roof}} = 201.86$ mm
- $d_{2,\text{roof}} = 224.01$ mm

where $d_{1,\text{roof}}$ and $d_{2,\text{roof}}$ are the lateral displacements at top of the building for TCS system and NSCS system, respectively.

By FE simulation of SPO process, global lateral deformation of structure can be calculated. Considering IDR as deformation performance parameter, maximum IDR for TCS and NSCS system are 1/247 (12.12 mm) and 1/214 (14.01 mm), respectively. In addition, IDR results under medium considered earthquake level are 1/357 (8.40 mm) for TCS system, and 1/291 (10.30 mm) for NSCS system.

Generally, NSCS system performs larger IDR response compared to TCS system, indicating less advantage in structural design. However, IDR is appropriate for damage assessments of multi-story buildings with shear deformation modes. For buildings with flexural deformation modes, especially high-rise buildings with shear wall system, IDR is not a proper parameter in evaluation, although it has been widely used as story-level performance parameter in codes and provisions. In high-rise building with flexural deformation mode, story rotation accumulates from bottom to top story, introducing rigid rotation angle in IDR with no story damage. For NSCS system, being typically flexural deformation mode, IDR may not be effective in performance evaluation, and detailed story damage evaluation should be carried out.

IV. Seismic Performance Evaluation

Seismic capacity of structure is evaluated by safety factor suggested in [9], [7], which represents for seismic design redundancy of structure. To calculate safety factor value, structure damage and ultimate state during pushover process should be studied. Considering shear walls are significant lateral resistant components in both TCS and NSCS systems, damage and failure of RC shear wall is focused on in this paper.

As discussed in Section III *C*, IDR is an inappropriate parameter for shear wall damage evaluation. To address this problem, various parameters have been presented in many researches and provisions for effective damage evaluation, such as effective IDR, harmful IDR, and other structural deformation parameters [8], [22], [23]. For RC shear wall components, suggested methods in Chinese provision CECS 392:2014 [7] and [8] have been respectively adopted in this paper, namely, (1) shear wall damage level based on material strain, and (2) shear wall damage state based on story curvature. The detailed application of these two methods is presented in following sections.

A. Damage Level based on Material Strain

In CECS 392:2014, different damage levels (from Lv.0 to Lv.6), dividing by different strain levels of concrete and rebar, are suggested in provisions for RC shear wall components under compressing-bending loads. For example, Lv.0 represents for no damage in RC shear wall, and strain of concrete and rebar are within elastic stage; Lv.6 represents for

failure in RC shear wall, ultimate strain is reached for either concrete or rebar.

In this study, for simplified expression, a normalized damage function D is defined, varying from 0 to 1, corresponding to damage level Lv.0 to Lv.6. Strain results of concrete and rebar in RC shear wall components can be obtained from FE models. By subroutine function *plotv* in *MSC.Marc* program, damage function D is calculated and presented in post process.

In Figs. 8 (a) and (b), ultimate states of TCS and NSCS systems are presented, indicating that the maximum value of damage function D in shear wall components first reaches 1 in the pushover process. It is implied that in both two systems, maximum shear wall damage exists in bottom stories, especially first story. At ultimate state, maximum damage at first story is Lv.6 (D = 1), whereas damage in upper stories is approximately Lv.0-Lv.1 (D < 0.1), indicating no damage or slight damage in shear wall. Compared to IDR distribution shown in Fig. 1, maximum IDR occurs at story 10 (for TCS system), and story 16 (for NSCS system). However, damage analysis proves that in those stories with large IDR value, damage is not severe, which is also consistent to general engineering seismic damage cases.

At ultimate state, shear wall damage distribution of first story is presented in Figs. 8 (c) and (d), and corresponding displacement at top of the structure is obtained, being 1047.9 mm for TCS system and 1512.6 mm for NSCS system.

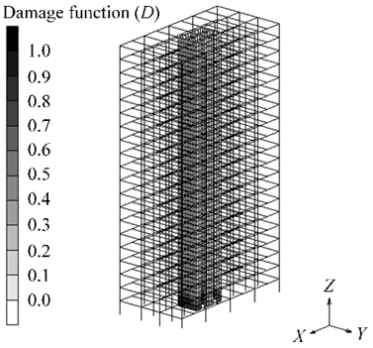

(a) TCS system

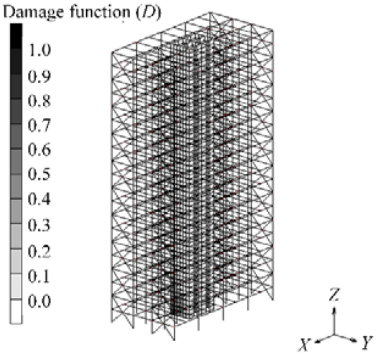

(b) NSCS system

Fig. 8 Shear wall damage distribution of two systems in ultimate state

B. Damage State based on Story Curvature

In addition of damage level parameter mentioned in Section IV *A*, another damage evaluation method using story curvature, proposed by [8], is also adopted in this study. According to different cross section strain states, damage states of shear wall component are defined: (1) DS1, being concrete cracking in tension; (2) DS2, being rebar yielding in tension; (3) DS3, being concrete crushing in compression. With plane section assumption, shear wall cross section strain distribution is shown in Fig. 9, and critical curvature values of 3 damage states can be calculated relatively.

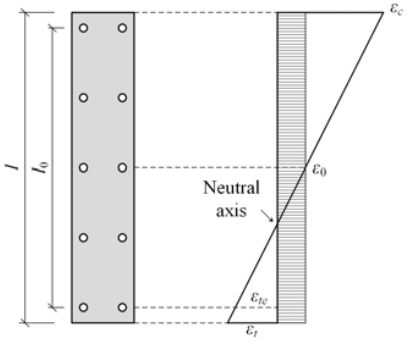

Fig. 9 Strain distribution of shear wall cross section

Considering shear wall as compressing-bending component, initial compressive strain caused induced by axial compression is

$$\varepsilon_0 = \mu \frac{f_c A_c + f_y A_s}{E_c A_c + E_s A_s} \tag{1}$$

where μ is axial compression ratio; f_c, f_y are relatively compressive strength of concrete, yield strength of rebar; A_c, A_s are relatively cross section area of concrete and rebar; E_c, E_s are relatively elastic modulus of concrete and rebar.

The tensile strain of concrete in tension should satisfy

$$\varepsilon_t = \frac{1}{2}\kappa l - \varepsilon_0 \tag{2}$$

and tensile strain of rebar is

$$\varepsilon_{te} = \frac{1}{2}\kappa l_0 - \varepsilon_0 \tag{3}$$

and compressive strain of concrete in compression is

$$\varepsilon_c = \frac{1}{2}\kappa l + \varepsilon_0 \tag{4}$$

where κ is curvature of shear wall component; l is cross section height; l_0 is core area height of cross section; ε_0, ε_t, ε_{te}, and ε_c are strains at different locations of cross section, as shown in Fig. 9.

Substitute critical strains related to each damage states into

(2)-(4), critical curvature of shear wall components can be calculated. For models of TCS and NSCS system in this paper, results are listed in Table IV.

TABLE IV
CRITICAL CURVATURE OF SHEAR WALL DAMAGE STATES

System	κ / (rad·mm^{-1})		
	DS1	*DS2*	*DS3*
TCS	1.16×10^{-7}	1.44×10^{-6}	2.62×10^{-6}
NSCS	1.56×10^{-7}	1.48×10^{-6}	2.58×10^{-6}

For structure cases in this paper, a mean story curvature value is obtained from displacement responses of FE models, as presented in Fig. 10 (taking story 1-3 at the bottom of structure as example). Generally, in both TCS and NSCS systems, with the increase of pushover displacement, mean curvature in bottom story increases, and shea0r wall damage state develops from initial state (no damage) to DS1-3. In TCS system, the value of mean curvature in story 1 is obviously larger than story 2 and 3, as well as the growing rate, indicating a concentrated damage in story 1. In NSCS system, curvature value in story 1-3 is close, and compared to TCS system, the growing rate of curvature is smaller, indicating a respectively slowly damage development in NSCS system.

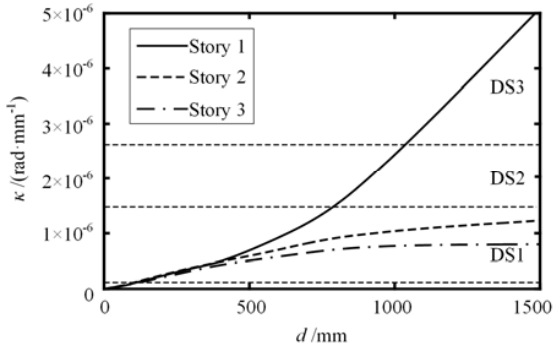

(a) TCS system

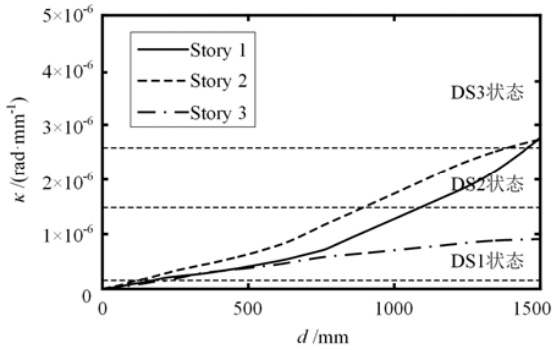

(b) NSCS system

Fig. 10 Mean story curvature variation of two systems

In story 10 and story 16, which are relatively stories with maximum IDR in TCS and NSCS systems, the value of mean curvature is much smaller than bottom stories, being 5.23×10^{-8} (TCS system) and 0.15×10^{-8} (NSCS system)(rad/mm), with damage state of shear wall components not exceed DS1. This implies that the stories with maximum IDR does not match with the stories with maximum shear wall damage, and it is also consistent with conclusion mentioned in Section IV *A*.

Considering DS3 (concrete crushing) as shear wall failure state, corresponding displacement at top of structure is 1040.2 mm (TCS system), 1460.0 mm (NSCS system).

C. Safety Factor

With acknowledgment of the structure damage and failure, safety factor of TCS and NSCS systems is calculated in this section, by [9]:

$$SF = \frac{a_c}{a_d} \tag{5}$$

where a_c is maximum peak ground acceleration capacity corresponding to ultimate state response of structure; a_d is elastic horizontal peak ground acceleration demand in design.

Incremental N2 method (IN2 method) is carried out to calculate a_c by [24]. Considering an increasing PGA of demand spectrum, the displacement response of SDOF system in SPO analysis increases by increment. At the step that the structural response meets ultimate state, the demand PGA equals to a_c.

Ultimate state of structure is defined as shear wall components failure in Section IV *A* and *B*. Fig. 11 presents the failure locations on pushover curves using strain and curvature criteria respectively (expressed by black and red circle spot). Two methods perform a consistent result in estimating structure ultimate state, with error of 0.60% (TCS system) and 3.48% (NSCS system). In following analysis, the ultimate state using strain criteria (black circle spot) are adopted.

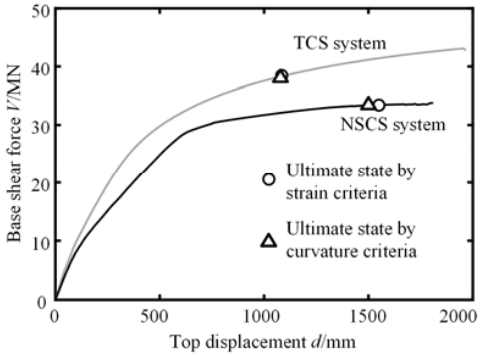

Fig. 11 Location of ultimate state in SPO process of two systems

In IN2 process, a simplified calculation method suggested in FEMA 273/274 [20], [21] is adopted. Inelastic spectrum displacement response is calculated by:

$$S_d = C_1C_2C_3S_{d,e} = C_1C_2C_3S_a\frac{T_e^2}{4\pi^2} \tag{6}$$

where S_{de} is elastic displacement response of SDOF system; T_e is elastic period of SDOF system; S_a is spectrum acceleration of

SDOF system corresponding to T_e; C_1, C_2, and C_3 are modification factors, valued according to FEMA 273/274 provisions: C_1 is modification factor to relate expected maximum inelastic displacements to displacements calculated for linear elastic response; C_2 represents the effect of stiffness degradation and strength deterioration on maximum displacement response; C_3 represents increased displacements due to dynamic P-Δ effects. The values of both C_2 and C_3 equal to 1.0 in this study.

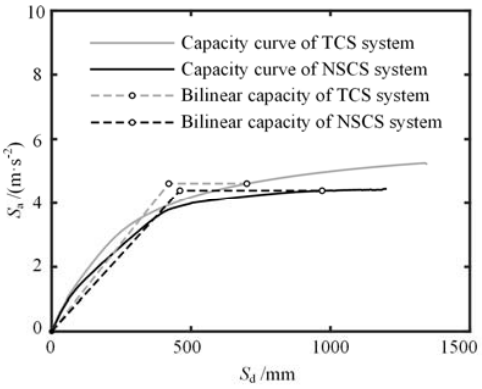

Fig. 12 Bilinear capacity curves of two systems

Bilinear capacity curves in the acceleration-displacement response spectrum (ADRS) format are plotted in Fig. 12, which are defined by three values: maximum spectral acceleration capacity (C_s) and yielding and maximum spectral displacement capacities (S_{dy} and S_{du} respectively). Based on bilinear capacity curves, elastic period of TCS and NSCS system are calculated respectively as 1.90s (TCS system) and 2.03s (NSCS system). Considering a Ru-u-T relationship suggested in EC8, C_1 is equal to 1.0 since T_e of both two systems value greater than ground period (T_g = 0.35s), and IN2 curves are obtained, as illustrated in Fig. 13. In both systems, IN2 curve takes a linear form, therefore a proportional spectrum is adopted, being demand corresponding to capacity curve at ultimate state of the structure, of which the peak ground acceleration is the value of a_c in (5). Finally, safety factors for TCS and NSCS systems are obtained, and calculation results are listed in Table V and Fig. 14.

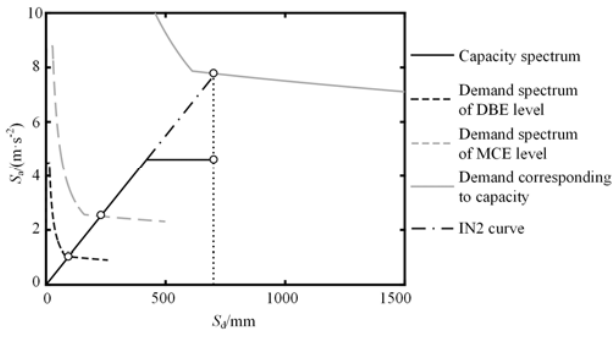

(a) TCS system

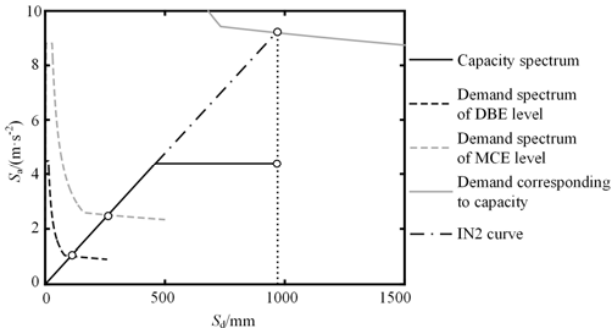

(b) NSCS system

Fig. 13 IN2 results and demand corresponding to capacity of two systems

TABLE V
PERFORMANCE PROPERTIES FOR TWO SYSTEMS

System	Earthquake level	S_{au}/ (m·s^{-2})	S_{dy}/ mm	S_{du}/ mm	a_c/ (m·s^{-2})	a_d/ (m·s^{-2})	SF
TCS	DBE	4.61	0.42	0.70	14.85	2.02	7.35
	MCE	4.61	0.42	0.70	14.85	3.97	3.74
NSCS	DBE	4.39	0.46	0.97	18.06	2.02	8.94
	MCE	4.39	0.46	0.97	18.06	3.97	4.55

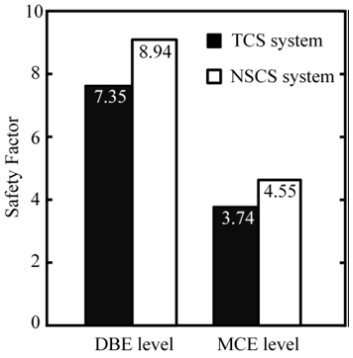

Fig. 14 Comparison of safety factor of two systems

In general, both TCS and NSCS systems perform a good redundancy under earthquake, and NSCS system shows greater global seismic capacities with respect to TCS system. SF of NSCS system is 21.6% higher than TCS system. This is mainly because of the damage plasticity development pattern of NSCS system. As exposed in Section III, NSCS system generally performs a lower plasticity development rate and a failure state with higher ductility, which leads to a higher failure displacement and PGA capacity of spectrum response.

D.Seismic Evaluation

An overall seismic evaluation using varied parameters is presented in Table VI, including global seismic response and damage in shear wall components.

It is presented that, though NSCS system performs a larger IDR response, shear wall components in TCS and NSCS systems are in the same damage state (damage level). Besides, the harmful IDR is calculated as IDR value with story rigid rotation accumulation eliminated. Therefore, harmful IDR

results also prove that NSCS system performs less shear wall damage. Safety factor indicates that NSCS system is more capable to bear higher seismic loads, thus under design demands, it is with more safety redundancy.

TABLE VI
SEISMIC EVALUATION AND COMPARISON OF TWO SYSTEMS

Performance indexes	DBE level		MCE level	
	TCS system	NSCS system	TCS system	NSCS system
IDR	1/357	1/291	1/247	1/214
Damage level [7]	Lv1	Lv1	Lv1	Lv1
Damage state [8]	DS1	DS1	DS1	DS1
Harmful IDR [23]	1/1613	1/3348	1/664	1/1572
Safety factor [9]	7.35	8.94	3.74	4.55

In general, composite structural system with separated gravity and lateral resistant systems is an innovation in assembly steel structure system with unique structure global mechanism and improved assembly efficiency. Specific design provisions for this structural system is still lacked in existing codes, but through static inelastic analysis and seismic evaluation, a close or even higher safety factor has been figured out in NSCS system compared to TCS system under the same IDR controlled level, indicating a practical engineering prospect.

V. CONCLUSION

Seismic evaluation of traditional composite frame-shear wall system and composite structural system with separated gravity and lateral resistant systems is carried out, aimed at seismic comparison of two structural systems under the same design controlled level. Static pushover method is adopted in FE analysis process, and varied parameters are used in evaluation based on computation results, including structure damage parameter, deformation parameter and safety factor. The inferred conclusions are as follows:

a. The separated composite structural system performs a lateral deformation of bending mode. During SPO process, main plasticity hinges exist in bottom ends of columns and braces. In comparison the separated composite structural system exhibits less plastic hinges and lower damage in shear wall components.
b. Both damage indexes based on story curvature and material strains are effective in shear wall damage evaluation. For separated composite structural system, damage mainly exists in bottom of the structure, especially story 1 to 3. In comparison, the separated composite structural system performs a relative lower damage development rate, indicated by story curvature results.
c. The new separated composite structural system performs a higher IDR response under DBE and MCE level, but a similar of even lower level in shear wall damage response. The safety factor value of separated composite structural system is higher than traditional composite structural system. The separated composite structural system is with higher seismic resistant ability and safety redundancy.

ACKNOWLEDGMENT

The authors gratefully acknowledge the financial support provided by the National Natural Science Foundation of China (Grant No. 51878378).

REFERENCES

[1] Z. Ni, "Research on bearing capacity performance of the truss girder in the modular prefabricated steel structure," *Industrial Construction*, vol. 44, no.8, pp. 14-18, 2014
[2] A. L. Zhang, "Pseudo dynamic tests for a resilient prefabricated prestressed steel frame," *Journal of Vibration and Shock,* vol. 35, no. 5, pp. 207-215, 2016.
[3] Y. L. Guo, "Design theory of assembled buckling-restrained braces and buckling-restrained braced frames," *Structural Engineers,* vol. 16, no.6, pp.164-176, 2010.
[4] X. C. Liu, "Experimental study on static and seismic performance of bolted joint in modularized multi-layer and high-rise prefabricated steel structures," *Journal of Building Structures,* vol. 36, no. 12, pp.43-51, 2015.
[5] J. P. Hao, "Research and applications of prefabricated steel structure building systems," *Engineering Mechanics,* vol.34, no.1, pp. 1-13, 2017.
[6] Y. B. Li, "Experiment on seismic performance of bundled lipped channel-concrete composite wall and beam-flange-strengthened connections," *Journal of Tianjin University,* vol.49, no.S1, pp.41-47, 2016.
[7] "Code for anti-collapse design of building structures: CECS 392:2014", Beijing, China Planning Press, 2014.
[8] C. Xiong, "Damage assessment of shear wall components for RC frame–shear wall buildings using story curvature as engineering demand parameter," *Engineering Structure,* vol.189, no.12, pp.77-88, 2019.
[9] F. G. Martínez, "Flavia De Luca, Gerardo M. Verderame. Seismic performances and behaviour factor of wide-beam and deep-beam RC frames," *Engineering Structures,* vol.125, no.20, pp.107-123, 2016.
[10] "Code for seismic design of buildings:GB 50011-2010", Beijing, China Architecture & Building Press, 2010.
[11] "Code for design of composite structures: JGJ 138-2016", Beijing, China Architecture & Building Press, 2016.
[12] M. X. Tao, "Theory of seismic response analysis of steel-concrete composite structures using fiber beam elements" *Journal of Building Structures,* vol. 32, no.10, pp.1-10, 2011.
[13] M. X. Tao, "Application of seismic response analysis of steel-concrete composite structures using fiber beam elements" *Journal of Building Structures,* vol. 32, no.10, pp.11-20, 2011.
[14] Z. W. Miao, "Applications of the multi-layer shell element in the finite element analysis of shear wall structures," in *Proceedings of 9th National Academic Conference on basic Theory and Engineering Application of Concrete Structure,* Beijing, pp.932-935, 2006.
[15] Rusch H. "Researches toward a general flexural theory for structural concrete," *Journal of the American Concrete Institute,* vol.57, no.7, pp.1-28, 1960.
[16] Esmaeily A. "Behavior of reinforced concrete columns under variable axial loads: analysis," *ACI Structural Journal*," vol.102, no.5, pp.736-744, 2005.
[17] Y. L. Huang, "A pushover analysis algorithm based on multiple point constraints," *Engineering Mechanics*, vol.28, no.2, pp.18-23, 2011.
[18] "Seismic Evaluation and Retrofit of Concrete Buildings, Volume1: ATC-40", California: Applied Technology Council, 1996
[19] X. Z. Lu, "Elasto-plastic analysis of buildings against earthquake – theory model and implementation on ABAQUS, MSC.MARC and SAP2000," Beijing: China Architecture & Building Press. 2009,"
[20] FEMA. NEHRP Guidelines for the Seismic Rehabilitation of Buildings: FEMA-273, Washington DC: Federal Emergency Management Agency; 1997.
[21] FEMA. NEHRP Commentary on the Guidelines for the Seismic Rehabilitation of Buildings: FEMA-274, Washington DC: Federal Emergency Management Agency, 1997.
[22] FEMA. Seismic performance assessment of buildings: Volume 1 : Methodology: FEMA P-58-1. Washington DC: Federal Emergency Management Agency; 2012.
[23] X. D. Ji, "Seismic performance evaluation of a high-rise building with novel hybrid coupled walls," Engineering Structures, vol.169, no.16, pp.216-225, 2018.

[24] M. Dolšek, "IN2 – A simple alternative for IDA," in *13th World Conference on Earthquake Engineering*. Vancouver, Canada: Canadian Association for Earthquake Engineering, pp.1-15, 2004.